Percolation phenomenon on fluorinated water in oil microemulsions: The effect of temperature

M. Grazia Giri, Marcello Carlà, Cecilia M.C. Gambi, and Donatella Senatra
Department of Physics, University of Florence, Largo Enrico Fermi 2, 50125 Florence, Italy

A. Chittofrati and A. Sanguineti
Ausimont, R&D Centre, Colloid Laboratory, Via San Pietro 50, 20021 Bollate, Milan, Italy
(Received 15 February 1994)

The static dielectric constant and the conductivity versus temperature were studied on a water in oil microemulsion composed of perfluoropolyether (PFPE) oil and surfactant at a constant water to surfactant ratio for different oil to surfactant ratios. The evidence of a percolation phenomenon is shown. An analysis in terms of scaling laws and a calculation of the scaling exponents indicate a dynamic percolation process below the threshold for all of the samples studied and above the threshold, far from phase transition regions. The exponents of static percolation are found above the threshold, close to the phase transition.

PACS number(s): 61.25.Hq, 64.70.Ja, 77.22.−d, 82.70.Dd

Percolation phenomena have been observed in various water in oil and in waterless microemulsions, both ternary and quaternary, composed of hydrogenated oil and surfactant [1–6]. For example, the water–sodium bis(2-ethylhexyl) sulfosuccinate (AOT)–oil ternary system, widely investigated for different oils, in some cases obeys the dynamic model of percolation of spheres within a continuous medium [2–5] as the percolative exponent below threshold, −1.2, differs from the value of the static case, −0.7 (bicontinuous structure). Such a result is related to the existence of spherical droplets, with attractive interactions, which exist up to a high volume fraction of the dispersed phase, ϕ =(water plus surfactant)/(total). To establish the structure of the system, accurate structural investigations at different temperatures throughout the monophasic region of the phase diagram were done, especially by small-angle neutron scattering (SANS) [7]. Glycerol (or formamide)-AOT-oil ternary systems as well as quaternary water–sodium dodecyl sulfate (SDS)–butanol–toluene systems also show dynamic percolation [6]. Furthermore the transition from dynamic percolation to static percolation, as well as the transition towards a lamellar phase, at the percolation threshold, was found in water-AOT-decane microemulsions [8]. Nonpercolative microemulsions showing large variations of conductivity were also evidenced in the brine–oil–nonionic amphiphile C_iE_j (polyglycolethers) system [9]. Conductivity measurements have been largely used to characterize fluorinated microemulsions [10–12]. However, only one conductivity curve with a percolative-like trend can be found in the literature [12] without any data analysis. So far, the dielectric properties of fluorinated microemulsions have not been studied to our knowledge. Nevertheless, the knowledge of dielectric parameters of such systems is of notable relevance. As a matter of fact, fluorinated surfactants are more suitable than the hydrogenated ones in reducing the surface tension [13], possess a higher chemical and thermal stability [13], and are able to solubilize gases in large amount [14]; they are used for industrial [15] as well as for biological applications [10,16].

In this paper we report the dielectric study of a water–fluorinated surfactant–fluorinated oil microemulsion where the fluorinated components are perfluoropolyethers (called PFPEs) manufactured by Ausimont S.p.A. (Milan, Italy). They are obtained by distillation under reduced pressure of industrial PFPEs (prepared by uv photoinitiated oxidation of perfluoropropene [17]) and have the main properties of fluorocarbons with the fluorocarbon chain rigidity reduced by the etheric bridges (C—O—C), which allows the liquid state up to molecular weights of 10 000 or more, increasing also the liquid state thermal range. A thorough description of the above compounds is in [18]. PFPEs have the following general formula:

$$R_e\text{—(O—CF}_2\text{—CF)}_n\text{—OCF}_2\text{—}R_h \qquad (1)$$
$$\qquad\qquad\qquad\quad |$$
$$\qquad\qquad\qquad \text{CF}_3$$

where R_e and R_h, oil chain ends, are a mixture of $—CF_3$, $—CF_3CF_2$ and $(CF_3)CF$ groups. The surfactant polar head group R_h is $—COO^-NH_4{}^+$. The oil has molecular weight (MW) 900 [19], density 1.8 g/cm^3, and viscosity 6.2 cp. The surfactant has MW 710 (MW distribution 95% by gas chromatographic analysis); the molecule length is 13 Å [21]. The ternary system of this work shows a large monophasic domain at $T = 20\,°C$, reported in Fig. 1, which shrinks towards the surfactant-oil side for higher temperatures [18]. Water and oil are insoluble in any proportions; water and surfactant give liquid crystalline phases [21,22]; the surfactant and the oil solubilize each other only at temperatures above 30 °C. Water droplets on a nanometer scale were identified by dynamic light scattering [23] (static light scattering confirmed these results [20,23]) at water to surfactant (W/S) molar ratio higher than 6. It was experimentally established that for low oil content, the droplets main-

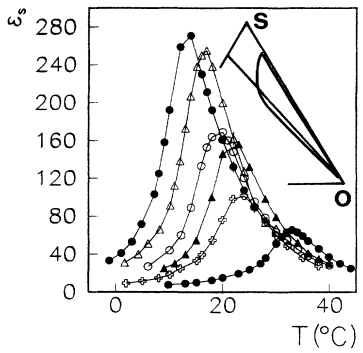

FIG. 1. The curves represent $\epsilon_s(T)$ at different ϕ values: full circles at $\phi = 0.501$ (highest curve) and $\phi = 0.205$ (lowest curve), open triangles at $\phi = 0.462$, open circles at $\phi = 0.395$, full triangles at $\phi = 0.361$, and open crosses at $\phi = 0.327$. For all the figures the error bars are not drawn when smaller than the symbols. Right top corner: the monophasic domain of the system at $T = 20\,°C$. The experimental path along the line $W/S = 11$ is also shown.

tain a constant radius at constant W/S. The second virial coefficient α was found < -20 at $W/S = 6.5$, -8 at $W/S = 11$ and -2 at $W/S = 16$. The hydrodynamic radius also increases from 3 to 6 nm as the W/S ratio increases. Spherical shapes were hypothesized in the dilute region as no experimental evidence of depolarized light was found and the polydispersity was very low (0.08–0.10). Water self-diffusion coefficients measured by pulsed gradient spin-echo (PGSE) NMR [24] indicated the existence of a water continuous network at $W/S \simeq 6.5$, which progressively disconnects upon addition of water at oil to surfactant (O/S) constant ratios (wt/wt) from 1.22 to 3.0. Conductivity measurements [20] at O/S constant ratios (wt/wt) from 1.22 to 5.67, performed as a function of water addition, allowed the detection of the transition from solution of hydrated surfactant species to real water in oil droplets. The minimum ratio W/S for which all the water molecules are inside the droplets was found to depend on the O/S ratios [20]. The surfactant used in [23,24] has a molecular weight 723, a little higher than that used in this paper and in [18,20]; as a consequence, the monophasic region was found slightly larger. The temperature of the experiments was 25 °C. No structural investigation has been done at $O/S \geq 1$ nor at high ϕ values (concentrated region) or at temperatures different from 25 °C. The interpretation of the light scattering results outside the dilute region presents some difficulties [23]. SANS preliminary experiments were done at $W/S = 11$ and $T = 25\,°C$ [22] in the concentrated region (no signal was detected in the dilute one); a broad peak is displayed in the scattering wave vector range 0–0.25 $Å^{-1}$ and the maximum intensity increases as a function of ϕ. Data analysis is in progress. The dielectric investigation allows the study of PFPE water in oil microemulsions throughout both the dilute and the concentrated regions leading, in a given experimental run, to the detection of both the Ohmic conductivity and the dielectric constant at different temperatures and frequencies. The apparatus and procedure used are described in [25]. For the measurements of this work the temperature was controlled within $\pm 0.05\,°C$. The samples exhibit dielectric absorption in the frequency range typical of microemulsions [25]. The analysis as a function of frequency, concentration, and temperature distinguishes percolative and nonpercolative regions and static or dynamic percolation. In this work we report the behavior of the static dielectric constant ϵ_s and of the conductivity σ along the line $W/S = 11$, in the thermal range in which the system is monophasic (see Figs. 1 and 2). The Hanai model [26] and the charge fluctuation model [27], which both consider the system composed of noninteracting hard spheres, predict, respectively, the following ϵ_s and σ values; ϵ_s up to 4 and σ up to 10^{-5} at the lowest ϕ of this work, 0.2; ϵ_s up to 16 and σ up to 5×10^{-5} at the highest ϕ of this work, 0.5. Only a few points of Fig. 1 and 2 at lowest ϕ and lowest temperature are justified by these models. The large jumps in ϵ_s and σ (See Figs. 1 and 2) were analyzed in terms of percolation theory as a percolation threshold was found for each curve. The microemulsion complex permittivity ϵ^* may be assumed a function of ϵ_1^* (dispersed water phase), ϵ_2^* (continuous oil phase), ϕ, and of the parameters containing all the information on the dispersion geometry and interactions [4]. $\epsilon_i^* = \epsilon_{is} - j\sigma_i/(\omega\epsilon_0)$ for $i = 1, 2$ where s means static, ϵ_0 is the permittivity of vacuum, $\omega = 2\pi f$, and f is the frequency. PFPE oil has $\sigma_2 \simeq 0$ and $\epsilon_2 = 1.8$ for frequencies up to 100 MHz (upper limit of the experimental apparatus). In the frequency range studied water and PFPE oil do not exhibit dielectric absorption; thus $|\epsilon_1^*| \gg |\epsilon_2^*|$, and in the presence of a percolation transition ϵ^* follows power laws as a function of both $|\phi - \phi_p|$ and $|T - T_p|$, characterized by exponents depending only on the dimensionality of the space (ϕ_p and T_p represent concentration and thermal percolation thresholds). As a function of temperature, at $T < T_p$, $\epsilon_s = c_2\epsilon_{2s}(T_p - T)^{-s}$ and $\sigma = c_2\sigma_2(T_p - T)^{-s}$; at $T > T_p$, $\epsilon_s = c_1\epsilon_{2s}(T - T_p)^{-s}$ and $\sigma = c_1\sigma_1(T - T_p)^{\mu}$. The exponents s and μ define the kind of percolation whether static or dynamic. In both cases $\mu = 1.5$–2.0; on the contrary, for static percolation $s = 0.6$–0.7 whereas for dynamic percolation $s \sim 1.2$ (see

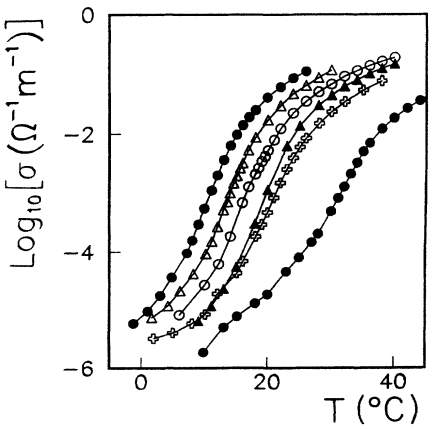

FIG. 2. $\sigma(T)$ at $W/S = 11$ for the same ϕ values as Fig. 1 with identical symbol meaning.

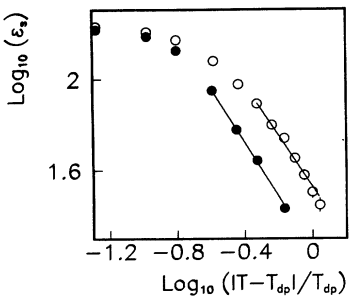

FIG. 3. An example of application of the scaling laws on the $\epsilon_s(T)$ curve below (full circles) and above (open circles) T_{dp}, at $\phi = 0.395$.

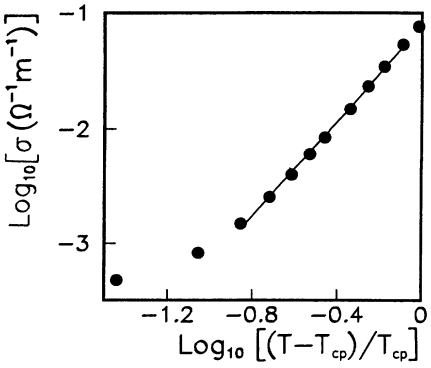

FIG. 4. Application of the scaling law to the points above threshold at $\phi = 0.327$.

[4] and the literature there reported).

The trend of ϵ_s vs temperature is shown in Fig. 1. The temperature corresponding to the maximum of ϵ_s represents the dielectric thermal percolation threshold T_{dp}. For each sample, in temperature intervals below and above threshold and slightly apart from the threshold, the function $\log_{10}(\epsilon_s)$ vs $\log_{10}(|T - T_{dp}|/T_{dp})$ follows a linear trend, as shown in Fig. 3 for $\phi = 0.395$ where the slope of the straight lines, s, is identical in both cases. In Table I, s_b (below threshold), s_a (above threshold), and T_{dp} are reported for all the samples. For what concerns the conductivity, for each sample, the function $\log_{10}[\sigma\ (\Omega^{-1}\,m^{-1})]$ vs T follows the trend shown in Fig. 2. The temperature of the curve inflection point is the conductivity thermal percolation threshold T_{cp}. In Fig. 4 the function $\log_{10}[\sigma\ (\Omega^{-1}m^{-1})]$ vs $\log_{10}[(T - T_{cp})/T_{cp})]$ of the data above threshold at $\phi = 0.327$, reported in Fig. 2, is drawn. A temperature interval within which the trend is linear is found and the exponent μ of the scaling law calculated. The T_{cp} and μ values are reported in Table I for all the samples. The analysis below T_{cp} does not allow an accurate calculation of the s exponent (for σ values lower than $10^{-4}\Omega^{-1}\,m^{-1}$ any small impurity may affect the measurements). However, the available data exclude s values lower than 1.1. From the $\epsilon_s(T)$ and $\sigma(T)$ curves, values of s and μ typical of dynamic percolation were found except for the extreme ϕ values above threshold. In the latter case, s_a values typical of static percolation were found. On the basis of the dielectric analysis the following can be argued. (i) Approaching the threshold from below, for all the samples studied, the system is composed of interacting droplets which form clusters of water droplets sufficiently close to each other so that a transfer of charge carriers between them can occur. At threshold, at least one cluster connects the system from one electrode to the other. (ii) Above threshold, in the central part of the line, as the temperature increases, water droplets form a growing number of water droplet clusters, by increasing the connectedness of the system. (iii) Above threshold, at the line extremes, i.e., in proximity to phase transition regions, the system behaves as a bicontinuous microemulsion; thus at the percolation threshold the coalescence of droplets begins, leading to the formation of continuous water channels whose number increases as the temperature increases. We discuss the above hypothesis in relation to the previous findings obtained at $W/S = 11$ and $T = 25\,^{\circ}C$. Point (i) is already confirmed by light scattering in the dilute region $\phi \leq 0.1$, as spherical droplets of 3.1 nm interact via an attractive potential, $\alpha = -8$ [23]. At these ϕ values, 25 °C is a temperature lower than the percolation threshold, as we expect that the trend $T_p(\phi)$ of Table I (T_p increases as ϕ decreases) is maintained also at the lowest ϕ of the line. The SANS spectra [22] on concentrated samples ($\phi \geq 0.4$) show an intensity peak which could be related to interacting droplets, confirming the points (i) and (ii). Conductivity [20] and NMR [24], which cover the range $\phi = 0.21$–0.55 and 0.33–0.55, respectively, agree in describing the system as intermediate between a continuous network [detected at $W/S = 6.5$ and corresponding

TABLE I. Dielectric and conductive percolative exponents and temperature thresholds for the samples at W/S=11 with different ϕ values. The errors are standard deviations. In data analysis χ^2 values close to 1 were found.

ϕ	s_b	s_a	T_{dp} (°C)	μ	T_{cp} (°C)
0.205	1.17 ± 0.02	0.83 ± 0.07	32.4 ± 0.2	1.495 ± 0.005	32.5 ± 0.2
0.327	1.28 ± 0.02	0.76 ± 0.03	22.8 ± 0.3	2.151 ± 0.004	19.3 ± 0.3
0.361	1.21 ± 0.02	1.17 ± 0.06	21.6 ± 0.2	1.819 ± 0.004	19.5 ± 0.3
0.395	1.18 ± 0.02	1.14 ± 0.04	18.9 ± 0.1	1.928 ± 0.005	16.5 ± 0.3
0.462	1.25 ± 0.01	1.13 ± 0.06	16.5 ± 0.1	2.227 ± 0.003	12.5 ± 0.3
0.501	1.19 ± 0.02	0.75 ± 0.08	13.0 ± 0.2	2.295 ± 0.004	9.3 ± 0.3

to conductivity maxima in the $\sigma(\phi)$ curves at constant O/S ratios] and a well defined droplet dispersion (at $W/S > 11$). The dielectric study at 25 °C (see Table I) shows the occurrence of dynamic percolation for $\phi = 0.2$–0.46 and of static percolation at $\phi = 0.5$. From the $\sigma(\phi)$ curves of [20], along the $W/S = 11$ line, the σ value at $\phi = 0.5$ is the closest to the conductivity maximum. It is worth noting that structural investigation must be performed to test the above hypothesis throughout the thermal range in which the system is monophasic. However, the investigation of this paper has clarified that percolation occurs in PFPE microemulsions, as demonstrated by the occurrence of large thermal ranges in which percolative laws are detected (the ranges of Fig. 1 except two points at the lowest temperature for $\phi = 0.501$, one point at the highest temperature for $\phi > 0.205$, and obviously the regions in the proximity of the threshold). On the basis of the above findings, droplets seem to exist throughout large ϕ and T ranges in the composition and thermal interval in which dynamic percolation occurs both below and above threshold. The exponents provide support that a transition from dynamic to static percolation occurs at $\phi < 0.36$ and $\phi > 0.46$. As a matter of fact, in the region at high surfactant concentration, a further increase of dispersed phase at $T = 25$ °C leads to the formation of anisotropic liquid crystals in equilibrium with microemulsion [28,29]. The evolution of the system is in agreement with the analysis of [24] in terms of Ninham's surfactant parameter v/al (ratio between the tail volume and head group area, in the lamellar phase, multiplied by the length) that offers some explanation of the occurrence of droplets shaped by PFPE surfactant in oils of different molecular weight as well as of the reason why high molecular weight oils do not favour droplet formation.

We feel confident that the results shown in this paper offer further support to the view that percolation belongs to the class of universality phenomena. SDS, AOT, and PFPE surfactants are very different in chemical composition and steric hindrance (hydrogenated, single and double chain SDS and AOT, respectively, and fluorinated single chain PFPE); however, when mixed with suitable nonconducting oil and suitable dispersed liquid, the PFPE surfactant gives a dynamic percolating system like AOT or SDS and alcohol.

The authors acknowledge useful discussions on percolation theory with R. Livi and thank Dr. P. Gavezzotti for the preparation of surfactants. This work was supported by Ausimont S.p.A. and by MURST 40% and 60% funds. M.G. Giri thanks Ausimont for support during this research work.

[1] M. Lagues, R. Ober, and C. Taupin, J. Phys. (Paris) Lett. **39**, L487 (1978).
[2] M. A. van Dijk, Phys. Rev. Lett. **55**, 1003 (1985).
[3] S. Bhattacharya, J. P. Stokes, M. W. Kim, and J. S. Huang, Phys. Rev. Lett. **55**, 1884 (1985).
[4] J. Peyrelasse, M. Moha-Ouchane, and C. Boned, Phys. Rev. A **38**, 904 (1988).
[5] C. Cametti, P. Codastefano, P. Tartaglia, J. Rouch, and S. H. Chen, Phys. Rev. Lett. **64**, 1461 (1990); Phys. Rev. A **45**, R5358 (1992).
[6] J. Peyrelasse, C. Boned, and Z. Saidi, Phys. Rev. E **47**, 468 (1993); **47**, 3412 (1993).
[7] M. Kotlarchyk, S. H. Chen, J. S. Huang, and M. W. Kim, J. Phys. Chem. **86**, 3273 (1982); Phys. Rev. Lett. **53**, 941 (1984); Phys. Rev. A **29**, 2054 (1984).
[8] A. Di Biasio, C. Cametti, P. Codastefano, P. Tartaglia, J. Rouch, and S. H. Chen, Phys. Rev. E **47**, 4258 (1993).
[9] M. Kahlweit, G. Busse, and J. Winkler, J. Chem. Phys. **99**, 5605 (1993).
[10] C. Burger-Guerrisi and C. Tondre, J. Chim. Phys. Phys. Chim. Biol. **86**, 1405 (1989).
[11] C. Tondre *et al.*, in *Surfactants in Solution*, edited by K. L. Mittal and P. Bothorel (Plenum Press, New York, 1986), Vol. 6, p. 1345; I. Rico *et al.*, *ibid.*, p. 1397.
[12] I. Rico, and A. Lattes, J. Colloid Interface Sci. **102**, 285 (1984).
[13] K. Shinoda, M. Hato, and T. Hayashi, J. Phys. Chem. **76**, 909 (1972).
[14] M. J. Stebe, G. Serratrice, and J. J. Delpuech, J. Phys. Chem. **89**, 2837 (1985).
[15] *Preparation, Properties and Industrial Applications of Organofluorine Compounds*, edited by R. E. Banks (Ellis Harward Ltd., Chichester, 1982).
[16] C. Cecutti, A. Novelli, I. Rico and A. Lattes, J. Dispersion Sci. Technol. **11**, 115 (1990).
[17] G. Caporiccio, F. Burzio, G. Carniselli, and V. Biancardi, J. Colloid Interface Sci. **98**, 202 (1984).
[18] A. Chittofrati, D. Lenti, A. Sanguineti, M. Visca, C. M. C. Gambi, D. Senatra, and Z. Zhou, Colloids Surf. **41**, 45 (1989); Prog. Colloid Polymer Sci. **79**, 218 (1989).
[19] Recent measurements indicate a molecular weight of 900 instead of 800 as reported in [18,20].
[20] A. Chittofrati, A. Sanguineti, M. Visca, and N. Kallay, Colloids Surf. **63**, 219 (1992).
[21] G. Gebel, S. Ristori, B. Loppinet, and G. Martini, J. Phys. Chem. **97**, 8664 (1993).
[22] S. Ristori, Ph.D. thesis, University of Florence, 1993.
[23] A. Sanguineti, A. Chittofrati, D. Lenti, and M. Visca, J. Colloid Interface Sci. **155**, 402 (1993).
[24] M. Monduzzi, A. Chittofrati, and M. Visca, Langmuir **8**, 1278 (1992).
[25] M. G. Giri, M. Carlà, C. M. C. Gambi, D. Senatra, A. Chittofrati, and A. Sanguineti, Meas. Sci. Technol. **5**, 627 (1993).
[26] C. Boned, J. Peyrelasse, M. Clausse, B. Lagourette, J. Alliez, and L. Babin, Colloid Polym. Sci. **257**, 1073 (1979).
[27] N. Kallay and A. Chittofrati, J. Phys. Chem. **94**, 4755 (1990).
[28] M. Monduzzi, V. Boselli, and A. Chittofrati, J. Phys. Chem. (to be published).
[29] A. Chittofrati, V. Boselli, and S. Friberg, J. Dispersion Sci. Tech. (to be published).